Electrochimica Acta 113 (2013) 735–740

Contents lists available at ScienceDirect

Electrochimica Acta

journal homepage: www.elsevier.com/locate/electacta

Synthesis of carbon-supported titanium oxynitride nanoparticles as cathode catalyst for polymer electrolyte fuel cells

Mitsuharu Chisaka[a,*], Akimitsu Ishihara[b], Ken-ichiro Ota[b], Hirokazu Muramoto[c]

[a] Department of Electronics and Information Technology, Hirosaki University, 3 Bunkyo-cho, Hirosaki, Aomori 036-8561, Japan
[b] Green Hydrogen Research Center, Yokohama National University, Yokohama 240-8501, Japan
[c] Cooperative Research Facility Center, Toyohashi University of Technology, 1-1 Hibarigaoka, Tempaku, Toyohashi, Aichi 441-8580, Japan

ARTICLE INFO

Article history:
Received 22 October 2012
Received in revised form 24 May 2013
Accepted 10 June 2013
Available online 21 June 2013

Keywords:
Titanium oxynitride
Carbothermal reduction
TiO_2
ORR
PEFC

ABSTRACT

For use as the oxygen reduction reaction (ORR) catalyst in polymer electrolyte fuel cell cathodes, carbon-supported titanium oxynitride (TiO_xN_y-C) nanoparticles with a size of approximately 5 nm or less were synthesized without using NH_3 gas. A sol–gel route developed for the synthesis of pure rutile TiO_2 nanopowders was modified to prepare the carbon-supported titanium oxide nanoparticles (TiO_x-C). For the first time, N atoms were doped into TiO_x solely by heating TiO_x-C under an inexpensive N_2 atmosphere at 873 K for 3 h, which could be due to carbothermal reduction. The TiO_x-C powder was also heated under NH_3 gas at various temperatures (873–1273 K) and durations (3–30 h). This step resulted in the formation of a TiN phase irrespective of the heating conditions. Both N_2- and NH_3-treated TiO_xN_y-C did not crystallize well; however, the former showed a mass activity more than three times larger than that of the latter at 0.74 V versus the standard hydrogen electrode. Thus, titanium oxide nanoparticles doped with a small amount of N atoms are suggested to be responsible for catalyzing ORR in the case of N_2-treated TiO_xN_y-C.

1. Introduction

Polymer electrolyte fuel cells (PEFCs) have long been considered to be promising candidates for power sources in vehicles, stationary applications, and compact portable devices. Performance and cost targets for PEFCs depend on the type of application. For example, reducing the loading of platinum-group metal catalysts in vehicles is an urgent requirement [1]. In 2011, the U.S. Department of Energy set technical targets for the use of platinum-group metal catalysts by the year 2017: the anode plus cathode loading should be reduced to 0.125 mg cm^{-2} with a simultaneous increase in the platinum mass activity and durability [2]. Because oxygen reduction reaction (ORR) at the cathode is much slower than hydrogen oxidation reaction at the anode, reducing the loading of platinum-group metal catalyst in cathodes causes much more severe performance loss than reducing catalyst loading at anodes does [3]. Therefore, development of ORR catalysts with non-platinum-group metals is an attractive strategy to achieve the target.

As recently reported [4–6], some non-platinum-group metal catalysts composed of Fe, N, and C show remarkable initial-stage performance in a single cell. In particular, when all conditions except for the catalyst loadings are identical, a membrane electrode assembly prepared using the catalyst developed by Proietti et al. [6] at the cathode showed cell voltages similar to those obtained using carbon-supported platinum (Pt-C) cathodes at low current densities. However, the cell voltages obtained using the catalyst developed by Proietti et al. started to drop at around 0.5 A cm^{-2}, and the difference between them and the voltages obtained in cells with Pt-C cathodes increased with increasing current densities. As the particle size of the catalyst developed by Proietti et al. is generally several micrometers or more [7], the resulting catalyst layer thickness is ~100 μm [6], which is nearly 10 times larger than that of state-of-the-art Pt-C-based catalyst layers. Therefore, the cell voltage at higher current densities cannot be increased by simply increasing the catalyst loading. This leads to large mass-transportation losses, that is, ohmic losses and oxygen diffusion losses caused by the large catalyst layer thickness [7]. As pointed out elsewhere [1], a decrease in mass transportation losses is necessary not only for this type of catalysts but also for other types of non-platinum-group metal catalysts such as metal oxides, oxynitrides, and nitrides.

One of the strategies for reducing the catalyst layer thickness is decreasing the size of the constituent material, preferably to the nanometer scale, which is similar to the case of Pt in Pt-C catalysts. Nanosized non-platinum-group metal oxide, oxynitride, and nitride catalysts such as tantalum oxide [8,9], zirconium oxynitride [10], hafnium oxynitride [11–13], molybdenum nitride [14,15],

* Corresponding author. Tel.: +81 172 39 3559; fax: +81 172 39 3559.
E-mail addresses: chisaka@eit.hirosaki-u.ac.jp, chisaka@cc.hirosaki-u.ac.jp (M. Chisaka).

0013-4686/$ – see front matter © 2013 Elsevier Ltd. All rights reserved.
http://dx.doi.org/10.1016/j.electacta.2013.06.048

chromium nitride [16], tungsten nitride [17], and titanium nitride [18] have been supported on carbon black for use in acidic PEFC cathode environments. Among them, oxides and oxynitrides of groups 4 and 5 metals are particularly stable because they are insoluble in acidic media, as confirmed by leaching tests conducted using inductively coupled plasma atomic emission spectroscopy. Further, we recently found that the presence of N atoms is necessary for maximizing the ORR activity of hafnium oxynitride nanoparticle catalysts [13] and titanium oxynitride catalysts of various particle sizes (~20–200 nm) [19]. Therefore, the development of nanosized oxynitride catalyst particles of groups 4 and 5 metals is an attractive option. However, only two types of materials, namely, zirconium, and hafnium oxynitride nanoparticles supported on carbon black, have been investigated so far; their synthesis includes heat treatment under an NH_3 atmosphere [10–13].

In the present work, we report an inexpensive synthesis route for carbon-supported titanium oxynitride (TiO_xN_y-C) nanoparticles without using NH_3 gas. Titanium is the most abundant among groups 4 and 5 metals [20]. The promising activity of titanium oxides or oxynitrides with particle sizes of several tens of nanometers or more has recently been reported by several authors, including us [19,21,22] and Lee's group [23]. A sol–gel route developed for the synthesis of nanosized unsupported rutile TiO_2 powder [24] was modified for the synthesis of TiO_xN_y-C. The crystal structures, morphologies, and surface chemical states of the TiO_xN_y-C catalysts were evaluated using X-ray diffraction (XRD), field emission transmission electron microscopy (FE-TEM), and X-ray photoelectron spectroscopy (XPS), respectively. The electrochemical stability and ORR activity was evaluated using cyclic voltammograms (CVs) and rotating disk electrode (RDE) voltammograms, respectively.

2. Experimental

2.1. Synthesis of catalysts

The TiO_xN_y-C catalysts were synthesized via a sol–gel route developed for rutile-TiO_2 nanopowders [24], with the following three modifications: (i) the addition of carbon supports, (ii) the use of different drying/heating conditions, and (iii) the use of different heating atmospheres in order to avoid oxidation of carbon supports at high temperatures and to dope N into the titanium oxides.

First, as-received carbon black powder (Vulcan XC-72, Cabot Co., Japan), hereafter denoted as C, was refluxed with nitric acid for 6 h, washed with water, and dried overnight at 363 K. Second, the refluxed C powder was stirred in 0.5 mol dm^{-3} hydrochloric acid at 273 K; this was followed by the addition of cold titanium tetrachloride ($TiCl_4$, Kishida Chemical Co., Japan). Third, the temperature of the dispersion was increased to ~330 K for 5 h with continuous stirring to evaporate the solvents. Fourth, the powder was washed with water and dried overnight in an oven at 363 K. Finally, the obtained precursor powder was placed in an alumina boat and heated in a horizontal quartz tube furnace that was slowly evacuated and purged with N_2 gas. The temperature was increased at a heating rate of 500 K h^{-1} from room temperature to different high temperatures T; the T was then maintained for a variable time t and then reduced to room temperature without controlling the cooling rate. Below T, N_2 gas at a flow rate of 300 standard cubic centimeters per minute (sccm; 1 sccm = 1.67×10^{-8} m^3 s^{-1}) was used. At T, the following flowing gases were utilized to maintain different atmospheric conditions: N_2 introduced at 300 sccm or NH_3 introduced at 200 sccm. Under the fixed heating conditions of T = 873 K and t = 3 h, N_2 gas was used (hereafter referred to as N_2 treatment), whereas under the other conditions of T = 873–1223 K and t = 3–30 h, NH_3 gas was used (hereafter referred to as NH_3 treatment). The mass of the catalyst sample was measured before and after NH_3 treatment, and the mass loss, Δm, was calculated using the following equation:

$$\Delta m = \frac{100(m_i - m_f)}{m_i} \quad (1)$$

where m_i and m_f denote the sample mass before and after NH_3 treatment, respectively. Some of the precursor powder particles were oxidized in air above 973 K for 1 h to remove the carbon supports. By measuring the mass before and after oxidation and assuming that the remaining white powder after oxidation was composed of TiO_2, the mass fraction of TiO_x in the precursor powder was determined to be 4.4% (w/w).

2.2. Characterization

The morphology and crystal structure of the two catalysts heat-treated at 873 K for 3 h under the different gases were investigated by using a field emission transmission electron microscope (JEM-2100F, JEOL Co., Japan). The crystal structures were also analyzed by using an X-ray diffractometer (RINT-2200, Rigaku Co., Japan) with Cu Kα radiation generated at 40 kV and 30 mA in the 2θ range 10°–90° at a scan rate of 2° min^{-1}. The chemical states of the catalysts were analyzed using an X-ray photoelectron spectrometer (Quantera SXM, ULVAC-PHI, Inc., Japan) with an Al Kα X-ray source (1486.6 eV).

2.3. Electrochemical stability and ORR activity measurements

To evaluate the electrochemical stability and ORR activity of the catalysts, CVs and RDE voltammograms were generated. The catalysts were dispersed in isopropyl alcohol by sonication for 1200 s to obtain a slurry. The mass fraction of the catalysts in the slurry was 2.5%. Aliquots of the slurry with volumes of 3.6 and 6.4 mm^3 were dropped onto glassy carbon (GC) disk electrodes with a geometrical surface area (S) of 0.0707 cm^2 (diameter, φ, of 3 mm) and 0.1257 cm^2 (φ = 4 mm), respectively, to obtain a TiO_xN_y-C catalyst loading (mS^{-1}) of 1 mg cm^{-2}. Subsequently, the electrodes were air-dried at 318 K for at least 600 s. To achieve a stable catalyst coating of the GC surface, 2.0 and 3.6 mm^3 of a 0.5% Nafion solution [prepared by diluting a 5% w/w Nafion solution (510211, Sigma–Aldrich Co., U.S.A.) in ethanol] was dropped onto the surface of the GC disk electrodes with S = 0.0707 and 0.1257 cm^2, respectively. This step was followed again by air-drying at 318 K for at least 600 s. Prior to these catalyst coating treatments, the surface of the GC disk electrodes was polished with 1.0 and 0.05 μm alumina slurries, washed with water and acetone, and dried at 318 K in air.

Using a conventional three-electrode cell, electrochemical measurements were performed in 0.1 mol dm^{-3} H_2SO_4 at room temperature. The catalyst-coated GC disk electrode, carbon paper (TGP-H-120, Toray, Japan), and Ag/AgCl (3 mol dm^{-3} NaCl) electrode (RE-1B, BAS Co., Japan) were used as the working, counter, and reference electrode, respectively. The working electrode was set in a rotator (RRDE-3A, BAS Co., Japan). All working electrode potentials were referenced to the standard hydrogen electrode (SHE). Using a potentiostat (Model 606A, ALS Co., U.S.A. or Model 2323, BAS Co., Japan), the RDE voltammograms were recorded by applying a disk potential, E, in the range of 0.05–1.2 V at a scan rate of 5 mV s^{-1} and a rotation speed of 1500 rpm after bubbling with O_2 for 1800 s. CVs under a N_2 atmosphere were also recorded for identical E range at scan rates of 5 and 50 mV s^{-1}. The current per unit geometrical area of the GC disk electrode obtained under the N_2 atmosphere (i_N) subtracted from that under O_2 atmosphere (i_O) was assumed to be responsible for the ORR.

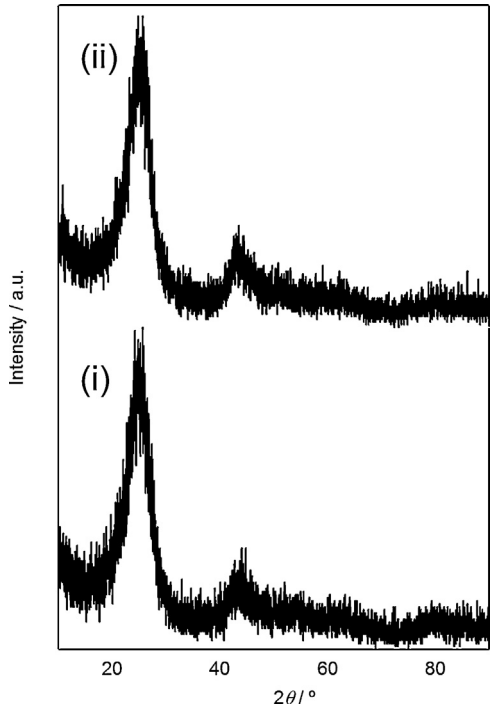

Fig. 1. XRD patterns of TiO_xN_y-C heat-treated at 873 K for 3 h under (i) N_2 and (ii) NH_3 gas.

The TiO_xN_y loading, m_TS^{-1}, of the NH_3-treated TiO_xN_y-C catalyst was calculated under the assumption that the mass loss during the NH_3 treatment was due to the gasification of C [25].

$$m_TS^{-1} = \frac{4.4}{100 - \Delta m} \quad (2)$$

3. Results and discussion

3.1. Crystal structure and morphology

The crystal structures and morphologies of the catalysts were evaluated by analyzing XRD patterns and FE-TEM images. Fig. 1 shows the XRD patterns of two types of TiO_xN_y-C catalysts: one synthesized by heating the precursor powder at $T = 873$ K for $t = 3$ h under flowing N_2 gas and the other under NH_3 gas. The two XRD patterns are almost identical and show the typical features of amorphous carbon black, indicating that the amount of titanium compounds was so small and/or amorphous that their peaks were not discernible because of the overlapping broad peaks of graphite.

Fig. 2 shows the corresponding FE-TEM images of these two catalysts. The titanium compound particles with a size of approximately 5 nm or less were supported on the surface of the C powder. No clear lattice fringe can be observed in Fig. 2(i), whereas weak fringes are discernible in Fig. 2(ii), suggesting that NH_3-treated TiO_xN_y particles crystallized to some extent. The lattice distance as calculated from the fringes was 0.21 nm, a typical value for the (2 0 0) plane in TiN. Further, the number of titanium compound nanoparticles in TiO_xN_y-C is lower than that of HfO_xN_y in HfO_xN_y-C [11–13]; we plan to increase this in our future studies.

3.2. Surface properties

Ti 2p and N 1s spectra of the precursor powder and TiO_xN_y-C catalysts heat-treated under N_2 at $T = 873$ K and $t = 3$ h, as well as those heat-treated under NH_3 at three different temperatures (873–1273 K) and two different durations (3 and 30 h), are shown in Fig. 3. The O 1s spectra were not examined in the present study because all samples contained contributions from functional groups on the C surface. It is well known that the Ti 2p level is spin–orbit split into the Ti $2p_{3/2}$ and Ti $2p_{1/2}$ sublevels, which can be seen in the Ti 2p spectra as a doublet. The precursor powder and N_2-treated TiO_xN_y-C showed a doublet at ~459.1 and ~465.0 eV, which are the typical values for fully oxidized Ti^{4+} in TiO_2 [26–31]. In the Ti $2p_{3/2}$ region of the Ti 2p spectra, peaks corresponding to Ti—N bonding in TiN (~455.2 eV [27,31]) or to O—Ti—N/Ti—O—N bonding in N-doped TiO_2 lattices or oxidized TiN (456–458 eV [26,27,29–31]) are absent in the N_2-treated TiO_xN_y-C spectrum [Fig. 3(II)], but are present in the spectra of the NH_3-treated catalysts [Fig. 3(III)–(VI)]. However, the N 1s spectra of the N_2-treated TiO_xN_y-C show weak peaks at ~401 and ~398 eV, indicative of O—Ti—N [26,29,30] and Ti—O—N [30] bonding, respectively, in the N-doped TiO_2 lattice [Fig. 3(II)]. These peaks could also be assigned to C—N bonding, because the binding energies of the two types of N functionalities in the N-doped carbon materials, the graphitic N and pyridinic N, are almost the same as those of O—Ti—N and Ti—O—N bonding, respectively [32]. However, N atoms are scarcely doped into the N-free C powder by heating under N_2 gas. Further, the fact that the precursor powder produced no such peaks at ~401 eV and ~398 eV in their N 1s spectrum [Fig. 3(I)] indicates that the C powder in TiO_xN_y-C was free from N. Therefore, the observed peaks in the N 1s spectrum shown in Fig. 3(II) should be assigned to O—Ti—N and Ti—O—N bonding in titanium oxynitride. We previously reported [12] that via carbothermal reduction, N atoms have been doped into hafnium oxide nanoparticles supported on carbon black prepared via a polymerized complex method by heat treatment under N_2 gas. This strategy has been often used to synthesize titanium oxy(carbo)nitride or TiN by heating a mixture of TiO_2 and carbon materials such as graphite and activated carbon under N_2 gas [33,34]. The results obtained from the XRD pattern [Fig. 1(i)], FE-TEM image [Fig. 2(i)], and XPS analysis [Fig. 3(II)] consistently indicate that amorphous TiO_2 nanoparticles doped with a small amount of N atoms were synthesized by heat treatment under N_2 gas, which proceeded as a result of carbothermal reduction.

The heat treatment of the precursor powder under NH_3 gas conditions identical to those employed in the heat treatment of TiO_xN_y-C under N_2 gas, i.e., $T = 873$ K and $t = 3$ h, resulted in the appearance of a new peak centered at 396–397 eV in the N 1s spectrum, as shown in Fig. 3(III). The new peak could be assigned to N—Ti—N bonding of stoichiometric TiN [26,27]. Further, the peak intensity increased with increasing T or t, as shown in Fig. 3(III)–(VI), suggesting the formation of an increasing amount of TiN during the NH_3 treatment.

A brief summary of the results discussed in the above two sections is given as follows: TiO_2 nanoparticles were successfully supported on carbon black; however, they were amorphous and/or the number of these nanoparticles was too low to be sufficient for their detection by XRD. They were doped with N by both N_2 and NH_3 treatment. The former treatment produced TiO_xN_y, possibly via carbothermal reduction, whereas the latter produced both TiO_xN_y and TiN.

3.3. Electrochemical stability and ORR activity

The electrochemical stability was evaluated using CVs obtained under the N_2 atmosphere at a scan rate of 50 mV s^{-1}. Fig. 4 shows the CVs of N_2-treated TiO_xN_y-C from the first to the 10th cycles. The CVs reached a steady state soon after the scan started. The anodic peak at ~0.54 V and the cathodic peak at ~0.41 V were stable during the 10 cycles, suggesting that they represented reversible reduction/oxidation (redox) couples. Because both the C supports and TiO_xN_y nanoparticles should contribute to the shape of CVs, the precise origin of these two peaks cannot be

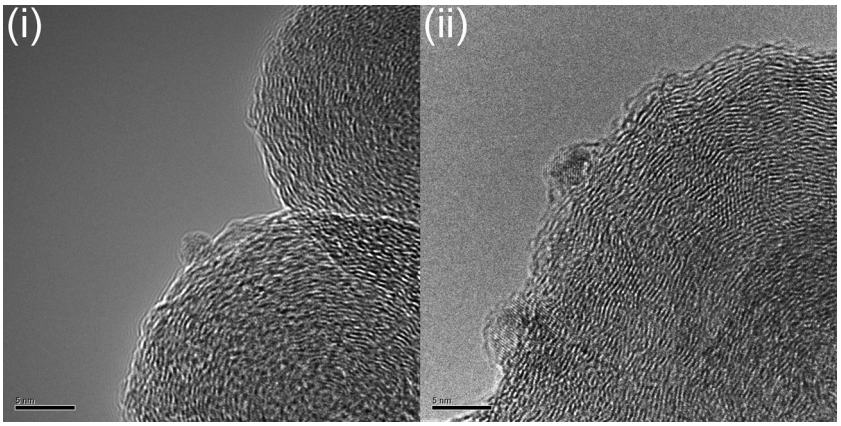

Fig. 2. FE-TEM images of TiO_xN_y-C heat-treated at 873 K for 3 h under (i) N_2 and (ii) NH_3 gas.

determined at present. However, the following two possible phases could be considered: (I) quinone/hydroquinone groups on the C surface, which show redox couples at ~0.6 V [35] and (II) rutile TiO_2, which shows a cathodic peak at ~0.4 V [21]. The N_2-treated TiO_xN_y-C was demonstrated to be electrochemically stable in acidic media because of the following two behaviors deduced from the CVs: they immediately reached a steady state and both the anodic and cathodic charges calculated from Fig. 4 were identical (3.9 mC). All the other catalysts showed similar behavior in their CVs.

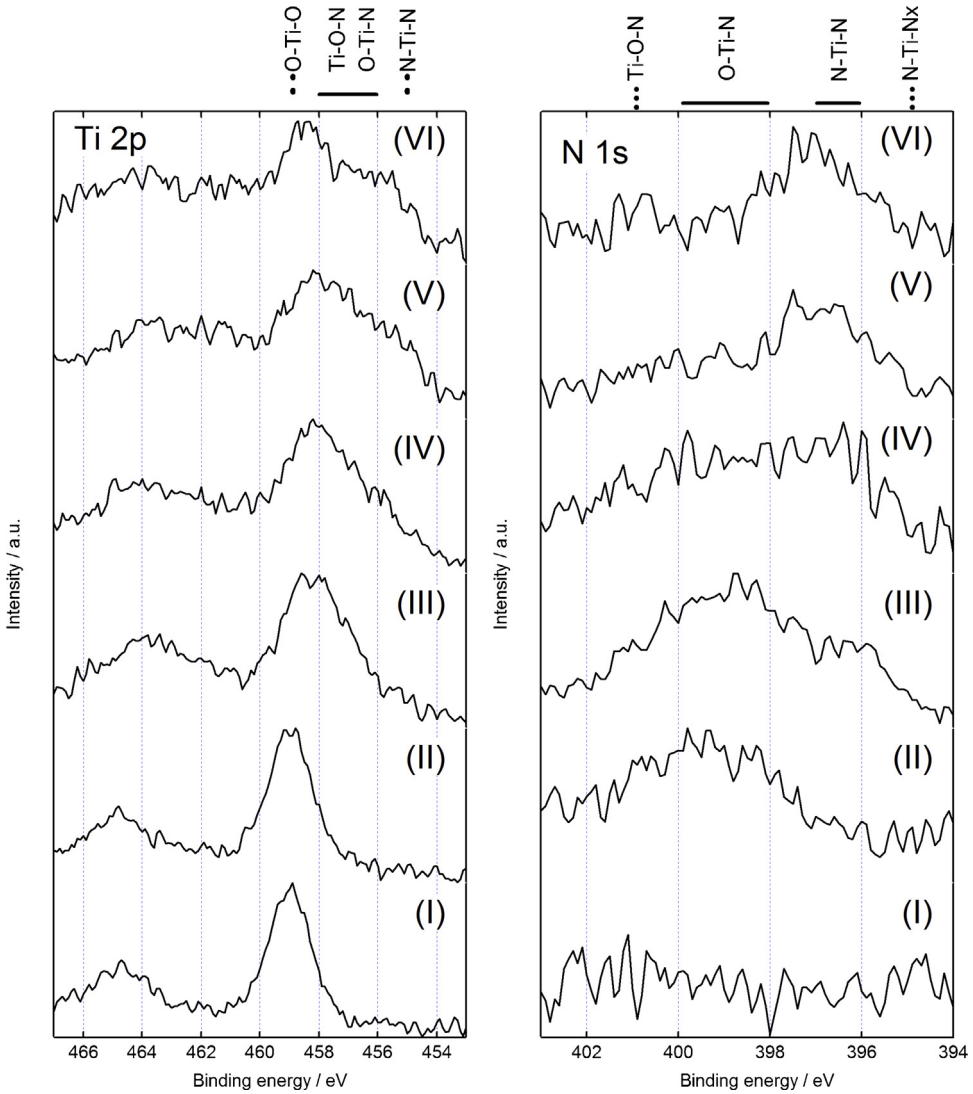

Fig. 3. Ti 2p and N 1s spectra of (I) the precursor powder; (II) TiO_xN_y-C heat-treated at 873 K for 3 h under N_2 gas; and TiO_xN_y-C heat-treated under NH_3 gas at (III) T = 873 K and t = 3 h, (IV) T = 1073 K and t = 3 h, (V) T = 1273 K and t = 3 h, and (VI) T = 1273 K and t = 30 h.

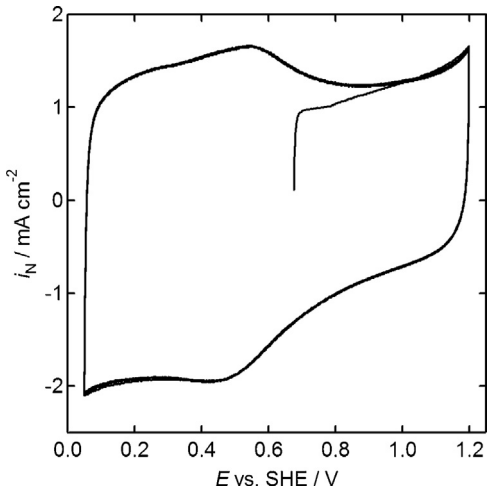

Fig. 4. CVs of TiO_xN_y-C heat-treated at 873 K for 3 h under N_2 gas. First to 10th scans presented were performed in 0.1 mol dm^{-3} H_2SO_4 under N_2 without rotations at a scan rate of 50 mV s^{-1}. The loading of TiO_xN_y-C, mS^{-1}, and corresponding TiO_xN_y loading, m_TS^{-1}, were 1 and 0.044 mg cm^{-2}, respectively.

Fig. 5 shows the RDE voltammogram of N_2-treated TiO_xN_y-C. Although this catalyst was synthesized without using NH_3 treatment, the ORR current density ($i_O - i_N$) appeared at around 0.8 V versus SHE. Because the TiO_xN_y loading (m_TS^{-1}) of NH_3-treated TiO_xN_y-C catalysts was not constant because of the difference in Δm (see Eq. (2)), the mass activity of TiO_xN_y, $-(I_O - I_N)m_T^{-1}$, was used to compare the activity of all catalysts. The value of the mass activity was evaluated at 0.74 V versus SHE, which corresponds to 0.8 V versus the reversible hydrogen electrode, at pH 1, which is commonly used by researchers [7]. At this potential, the contribution of C to the activity of NH_3-treated TiO_xN_y-C is assumed to be negligible at $T \leq 1223$ K and $t \leq 24$ h [36]. Fig. 6 shows the $-(I_O - I_N)m_T^{-1}$ of N_2- and NH_3-treated TiO_xN_y catalysts. N_2-treated TiO_xN_y-C showed the highest $-(I_O - I_N)m_T^{-1}$ value of 0.35 A g^{-1}, which is more than three times larger than that of any NH_3-treated TiO_xN_y-C catalyst. These results and the results from XPS analyses (Fig. 3) suggest that titanium oxide doped with a small amount of N is electrochemically stable and more active than TiN,

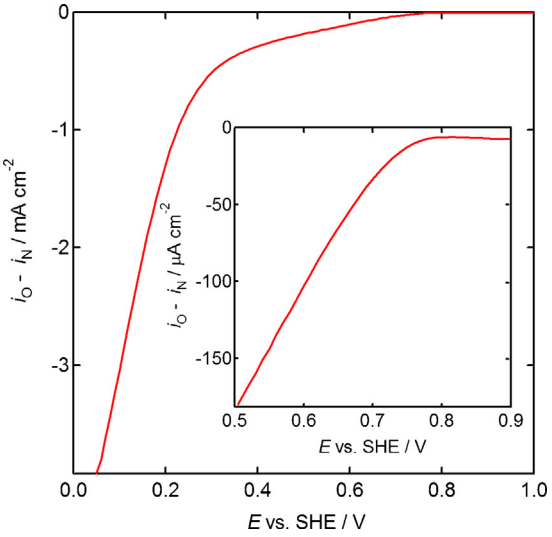

Fig. 5. RDE voltammogram of TiO_xN_y-C heat-treated at 873 K for 3 h under N_2 gas. Scans were performed in 0.1 mol dm^{-3} H_2SO_4 under N_2 without rotations and under O_2 with a rotation speed of 1500 rpm at a scan rate of 5 mV s^{-1}. The mS^{-1} and corresponding m_TS^{-1} were 1 and 0.044 mg cm^{-2}, respectively. The inset shows the voltammogram for $E \geq 0.5$ V vs. SHE.

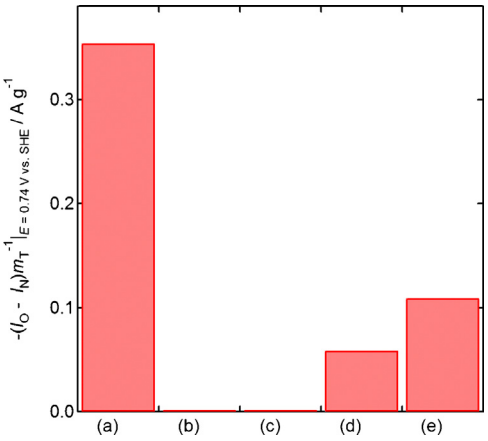

Fig. 6. Oxygen reduction reaction mass activity, $-(I_O - I_N)m_T^{-1}$ of (a) TiO_xN_y-C heat treated under N_2 gas at $T = 873$ K and $t = 3$ h and TiO_xN_y-C heat-treated under NH_3 gas at (b) $T = 873$ K and $t = 3$ h, (c) $T = 1073$ K and $t = 3$ h, (d) $T = 1273$ K and $t = 3$ h, and (e) $T = 1273$ K and $t = 30$ h.

in accordance with the trends observed in our previous study [19]. The maximum mass activity level achieved in this study is comparable to that of iron-based catalysts, which varies between 0.4 and 18 A g^{-1} [7]. This is the first report on such high mass activity of highly stable catalysts based on oxides of groups 4 and 5 metals. The synthesis route for nanosized group 4 or 5 metal oxynitride particles employed in this study was demonstrated to be promising for increasing the mass activity and for reducing the thickness of catalyst layers. Crystallinity and mass fraction of TiO_xN_y in TiO_xN_y-C are the key parameters for achieving further improvement.

4. Conclusions

A limited number of TiO_xN_y particles with a size of approximately 5 nm or less were successfully supported on carbon black for use as cathode catalyst in PEFCs. For the first time, N atoms were doped into TiO_x prepared via a sol–gel route solely by heating TiO_x under N_2 gas; the possible mechanism is assumed to be carbothermal reduction. The N_2-treated TiO_xN_y-C was electrochemically stable in 0.1 mol dm^{-3} H_2SO_4. Further, it showed a mass activity of 0.35 A g^{-1} at 0.74 V versus SHE, which was more than three times larger than that in any of the NH_3-treated TiO_xN_y-C catalysts. Because the NH_3-treatment resulted in the formation of TiN, which is not highly active toward ORR, TiO_x doped with a small amount of N was suggested to be responsible for the high ORR activity of the N_2-treated TiO_xN_y-C catalysts.

Acknowledgments

This work was partially supported by the Grant-in-Aid for Young Scientists (B), 23760185, from the Japanese Ministry of Education, Culture, Sports, Science and Technology and the Grant for Exploratory Research by Young Scientists from Hirosaki University.

References

[1] M.K. Debe, Electrocatalyst approaches and challenges for automotive fuel cells, Nature 486 (2012) 43.
[2] U.S. Department of Energy; Technical Plan-Fuel Cells, 2011, http://www1.eere.energy.gov/hydrogenandfuelcells/mypp/pdfs/fuel_cells.pdf; pp 3. 4–27 (accessed 23.09.12).
[3] H.A. Gasteiger, J.E. Panels, S.G. Yan, Dependence of PEM fuel cell performance on catalyst loading, Journal of Power Sources 127 (2004) 162.
[4] M. Lefevre, E. Proietti, F. Jaouen, J.P. Dodelet, Iron-based catalysts with improved oxygen reduction activity in polymer electrolyte fuel cells, Science 324 (2009) 71.

[5] G. Wu, K.L. More, C.M. Johnston, P. Zelenay, High-performance electrocatalysts for oxygen reduction derived from polyaniline, iron, and cobalt, Science 332 (2011) 443.
[6] E. Proietti, F. Jaouen, M. Lefevre, N. Larouche, J. Tian, J. Herranz, J.P. Dodelet, Iron-based cathode catalyst with enhanced power density in polymer electrolyte membrane fuel cells, Nature Communications 2 (2011) 416.
[7] F. Jaouen, J. Herranz, M. Lefevre, J.P. Dodelet, U.I. Kramm, I. Herrmann, P. Bogdanoff, J. Maruyama, T. Nagaoka, A. Garsuch, J.R. Dahn, T. Olson, S. Pylypenko, P. Atanassov, E.A. Ustinov, Cross-laboratory experimental study of non-noble metal electrocatalysts for the oxygen reduction reaction, ACS Applied Materials & Interfaces 1 (2009) 1623.
[8] J.Y. Kim, T.K. Oh, Y. Shin, J. Bonnett, K.S. Weil, A novel non-platinum group electrocatalyst for PEM fuel cell application, International Journal of Hydrogen Energy 36 (2011) 4557.
[9] J. Seo, D. Cha, K. Takanabe, J. Kubota, K. Domen, Highly-dispersed Ta-oxide catalysts prepared by electrodeposition in a non-aqueous plating bath for polymer electrolyte fuel cell cathodes, Chemical Communications 48 (2012) 9074.
[10] G. Liu, H. Zhang, M. Wang, H. Zhong, J. Chen, Preparation, characterization of ZrO_xN_y/C and its application in PEMFC as an electrocatalyst for oxygen reduction, Journal of Power Sources 172 (2007) 503.
[11] M. Chisaka, T. Iijima, T. Yaguchi, Y. Sakurai, Carbon-supported hafnium oxynitride as cathode catalyst for polymer electrolyte membrane fuel cells, Electrochimica Acta 56 (2011) 4581.
[12] M. Chisaka, Y. Suzuki, T. Iijima, Y. Sakurai, Effect of synthesis route on oxygen reduction reaction activity of carbon-supported hafnium oxynitride in acid media, Journal of Physical Chemistry C 115 (2011) 20610.
[13] M. Chisaka, Y. Suzuki, T. Iijima, Y. Ishihara, R. Inada, Y. Sakurai, Active sites for oxygen reduction reaction and the reaction mechanism in carbon-supported hafnium oxynitride, ECS Electrochemistry Letters 1 (2012) F4.
[14] H. Zhong, H. Zhang, G. Liu, Y. Liang, J. Hu, B. Yi, A novel non-noble electrocatalyst for PEM fuel cell based on molybdenum nitride, Electrochemistry Communications 8 (2006) 707.
[15] D. Xia, S. Liu, Z. Wang, G. Chen, L. Zhang, L. Zhang, S. Hui, J. Zhang, Methanol-tolerant MoN electrocatalyst synthesized through heat treatment of molybdenum tetraphenylporphyrin for four-electron oxygen reduction reaction, Journal of Power Sources 177 (2008) 296.
[16] H. Zhong, X. Chen, H. Zhang, M. Wang, S.S. Mao, Proton exchange membrane fuel cells with chromium nitride nanocrystals as electrocatalysts, Applied Physics Letters 91 (2007) 163103.
[17] H. Zhong, H. Zhang, Y. Liang, J. Zhang, M. Wang, X. Wang, A novel non-noble electrocatalyst for oxygen reduction in proton exchange membrane fuel cells, Journal of Power Sources 164 (2007) 572.
[18] J. Chen, K. Takanabe, R. Ohnishi, D. Lu, S. Okada, H. Hatasawa, H. Morioka, M. Antonietti, J. Kubota, K. Domen, Nano-sized TiN on carbon black as an efficient electrocatalyst for the oxygen reduction reaction prepared using an mpg-C_3N_4 template, Chemical Communications 46 (2010) 7492.
[19] M. Chisaka, A. Ishihara, K. Suito, K. Ota, K. Muramoto, Oxygen reduction reaction activity of nitrogen-doped titanium oxide in acid media, Electrochimica Acta 88 (2013) 697.
[20] Mineral Commodity Summaries, U.S. Geological Survey, 2012, http://minerals.usgs.gov/minerals/pubs/mcs/2012/mcs2012.pdf; pp. 174–175 (accessed 23.09.12).
[21] J.H. Kim, A. Ishihara, S. Mitsushima, N. Kamiya, K. Ota, Catalytic activity of titanium oxide for oxygen reduction reaction as a non-platinum catalyst for PEFC, Electrochimica Acta 52 (2007) 2492.
[22] Y. Ohgi, A. Ishihara, Y. Shibata, S. Mitsushima, K. Ota, Catalytic activity of partially oxidized transition-metal carbide–nitride for oxygen reduction reaction in sulfuric acid, Chemistry Letters 37 (2008) 608.
[23] D.T. Dam, K.D. Nam, H. Song, X. Wang, J.M. Lee, Partially oxidized titanium carbonitride as a non-noble catalyst for oxygen reduction reactions, International Journal of Hydrogen Energy 37 (2012) 15135.
[24] Q. Zhang, L. Gao, J. Guo, Effects of calcination on the photocatalytic properties of nanosized TiO_2 powders prepared by $TiCl_4$ hydrolysis, Applied Catalysis B: Environmental 26 (2000) 207.
[25] F. Jaouen, F. Charreteur, J.P. Dodelet, Fe-based catalysts for oxygen reduction in PEMFCs Importance of the disordered phase of the carbon support, Journal of Electrochemical Society 153 (2006) A689.
[26] K.S. Robinson, P.M.A. Sherwood, X-ray photoelectron spectroscopic studies of the surface of sputter ion plated films, Surface and Interface Analysis 6 (1984) 261.
[27] N.C. Saha, H.G. Tompkins, Titanium nitride oxidation chemistry: an X-ray photoelectron spectroscopy study, Journal of Applied Physics 72 (1992) 3072.
[28] S. Hashimoto, A. Miura, T. Sakurada, A. Tanaka, Alternation of Ti 2p XPS spectrum for TiO_2 by Ar ion bombardment, Journal of Surface Analysis 9 (2002) 459.
[29] X. Chen, C. Burda, Photoelectron spectroscopic investigation of nitrogen-doped titania nanoparticles, Journal of Physical Chemistry B 108 (2004) 15446.
[30] Y. Cheng, J. Zhang, F. Chen, M. Anpo, Synthesis and characterization of nitrogen-doped TiO_2 nanophotocatalyst with high visible light activity, Journal of Physical Chemistry C 111 (2007) 6979.
[31] B. Avasarala, T. Murray, W. Li, P. Haldar, Titanium nitride nanoparticles based electrocatalysts for proton exchange membrane fuel cells, Journal of Materials Chemistry 19 (2009) 1803.
[32] J.R. Pels, F. Kapteijin, J.A. Moulijn, Q. Zhu, K.M. Thomas, Evolution of nitrogen functionalities in carbonaceous materials during pyrolysis, Carbon 33 (1995) 1641.
[33] S.A. Rezan, G. Zhang, O. Ostrovski, Carbothermal reduction and nitridation of titanium dioxide in a H_2–N_2 gas mixture, Journal of the American Ceramic Society 94 (2011) 3804.
[34] A. Ortega, M.A. Roldan, C. Real, Carbothermal synthesis of titanium nitride (TiN): Kinetics and Mechanism, International Journal of Chemical Kinetics 37 (2005) 566.
[35] H. Gomathi, G. Prabhakara Rao, Chemical and electrochemical modification of the glassy carbon surface with quinhydrone, Journal of Electroanalytical Chemistry 190 (1985) 85.
[36] M. Chisaka, T. Iijima, A. Tomita, T. Yaguchi, Y. Sakurai, Oxygen reduction reaction activity of vulcan XC-72 doped with nitrogen under NH_3 gas in acid media, Journal of the Electrochemical Society 157 (2010) B1701.